JOURNAL OF MOLECULAR SPECTROSCOPY 167, 365–374 (1994)

Torsional Splitting in the $2\nu_9$ and ν_5 Vibrational Band of HNO_3

THOMAS M. GOYETTE,* CHRISTOPHER D. PAULSE,* LEE C. OESTERLING,* FRANK C. DE LUCIA,* AND PAUL HELMINGER†

*Department of Physics, The Ohio State University, Columbus, Ohio 43210; and †Department of Physics, University of South Alabama, Mobile, Alabama 36688

Torsional splittings in both the $2\nu_9$ and ν_5 vibrational states have been resolved and observed in the millimeter/submillimeter spectrum of HNO_3. The former splitting is due to the torsional motion of H around the NO bond in the ν_9 mode, whereas the latter is due to the large mixing which results from the near degeneracy (17.34 cm^{-1}) of the two vibrational modes. It is possible to use these data in the context of a very simple model to quantitatively *predict* the observed intensity of the $2\nu_9$ infrared band. Furthermore, these data remove the fitting indeterminacy which exists in the rotation–vibration data between the difference in the vibrational energy of the two states and the Fermi interaction term.

I. INTRODUCTION

The rotational–vibrational structure of HNO_3 has been extensively studied over the years both by microwave and infrared techniques (*1–3*). Of all of the bands, the complex $\nu_5/2\nu_9$ interacting dyad near 11 μm has drawn perhaps the most attention, both because of its intrinsic spectroscopic interest and its strength and convenient spectral location for remote sensing. The latter attribute has led to extensive study with atmospheric instruments of ever increasing spectral resolution (*4–10*).

Central to any consideration of this dyad is the strong interaction between these two vibrational bands that results from the small (17.34 cm^{-1} (*1, 2*)) splittings between their band origins. Among the manifestations of this interaction are large perturbations and significant correlations among derived constants. The latter can lead to considerable fitting indeterminacy and uncertainty in the physical interpretation of the parameters. Additionally, it has long been recognized that the observed strength of the $2\nu_9$ band (about 70% that of ν_5) is primarily due to its mixing with ν_5, rather than the intrinsic strength of the pure $2\nu_9$ overtone band (*1, 2*).

We have found that careful inspection of the millimeter/submillimeter (mm/submm) spectra of these two bands makes possible a direct measurement of this mixing, independent of correlations. Briefly, it is possible to resolve and observe relatively weak *b*-type transitions in the pure rotational bands of both $2\nu_9$ and ν_5 which are offset from the location of the stronger *a*-type transitions by torsional splitting; in the case of $2\nu_9$ the splitting is a direct result of the torsional motion around the NO bond whereas in ν_5 the observed splitting comes from the strong mixing of the states. The splitting in $2\nu_9$, especially for the higher values of K_+ where the splitting is largest, has been previously observed by infrared diode laser techniques (*2, 11*). The observation of both of these splittings provides an opportunity to *predict* the observed intensity of the $2\nu_9$ infrared band, as well as to separate the correlation between the vibrational terms and Fermi interaction terms which exists in the rotation–vibration spectrum.

0022-2852/94 $6.00

II. THEORY

The physics underlying the work described in this paper is particularly straightforward because it can be shown experimentally that the observed torsional splittings in both ν_5 and $2\nu_9$ are not strongly dependent on the rotational state (the relevant energy levels are shown in Fig. 1). The vibrational energy eigenvalues of ν_5 and $2\nu_9$ are obtained by diagonalizing

$$H = \begin{bmatrix} E^0_{2\nu_9} & W_{12} \\ W_{12} & E^0_{\nu_5} \end{bmatrix}, \tag{1}$$

where $E^0_{2\nu_9}$ and $E^0_{\nu_5}$ are the unperturbed vibrational energies and W_{12} is the Fermi resonance matrix element (*12, 13*). The similarity transformation yielding the eigenvalues dictates the form of the vibrational wavefunctions as

$$\psi_{2\nu_9} = \cos\theta\psi^0_{2\nu_9} + \sin\theta\psi^0_{\nu_5} \tag{2a}$$

$$\psi_{\nu_5} = -\sin\theta\psi^0_{2\nu_9} + \cos\theta\psi^0_{\nu_5}, \tag{2b}$$

where

$$\tan 2\theta = \frac{2W_{12}}{\Delta E^0} \quad \text{and} \quad \Delta E^0 = E^0_{2\nu_9} - E^0_{\nu_5}. \tag{3}$$

By introducing a torsional splitting 2δ into the $2\nu_9$ state, two vibrational Hamiltonians result

$$H_\pm = \begin{bmatrix} E^0_{2\nu_9} \pm \delta & W_{12} \\ W_{12} & E^0_{\nu_5} \end{bmatrix}, \tag{4}$$

with + and − signifying the upper and lower state. Diagonalizing this matrix and identifying torsional levels according to Fig. 1, the rotationless torsional splittings in ν_5 and $2\nu_9$ become

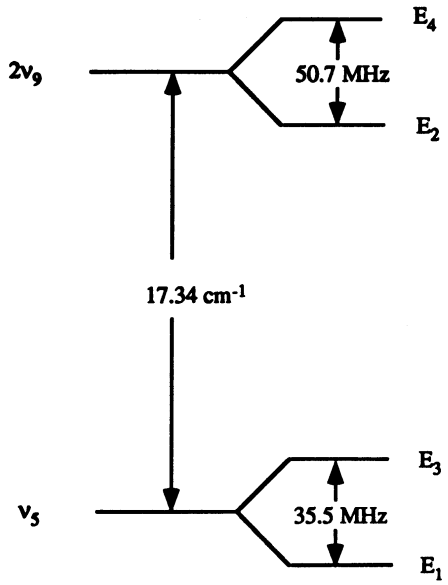

FIG. 1. Energy levels of the ν_5 and $2\nu_9$ interacting states.

$$E_3 - E_1 = \delta - \frac{1}{2}Q \tag{5a}$$

$$E_4 - E_2 = \delta + \frac{1}{2}Q \tag{5b}$$

and

$$\Delta E = \frac{1}{2}\sqrt{4W_{12}^2 + (\Delta E^0 + \delta)^2} + \frac{1}{2}\sqrt{4W_{12}^2 + (\Delta E^0 - \delta)^2}, \tag{5c}$$

where

$$Q = \sqrt{4W_{12}^2 + (\Delta E^0 + \delta)^2} - \sqrt{4W_{12}^2 + (\Delta E^0 - \delta)^2} \tag{6}$$

and $\Delta E = (E_4 + E_2)/2 - (E_3 + E_1)/2 \sim 17.34\ \text{cm}^{-1}$.

The relative intensities of the ν_5 and $2\nu_9$ infrared bands can be determined from the eigenvector coefficients of Eqs. (2a) and (2b) as

$$\frac{\Gamma_{\nu_5}}{\Gamma_{2\nu_9}} = \frac{1}{\tan^2\theta}. \tag{7}$$

Solving Eqs. (5) and (6), we find that

$$\Delta E^0 = \frac{Q}{2\delta}\Delta E \tag{8}$$

and

$$W_{12} = \frac{1}{4}\sqrt{\left[\left(4 - \frac{Q^2}{\delta^2}\right)\Delta E^2 + (Q^2 - 4\delta^2)\right]}. \tag{9}$$

Equation (3) then becomes

$$\theta = \frac{1}{2}\tan^{-1}\left(\frac{\delta}{Q}\sqrt{\left[\left(4 - \frac{Q^2}{\delta^2}\right) + \frac{Q^2 - 4\delta^2}{\Delta E^2}\right]}\right). \tag{10}$$

Since the splitting is so much smaller than the Fermi interaction, Eq. (7) becomes

$$\frac{\Gamma_{\nu_5}}{\Gamma_{2\nu_9}} = \frac{(E_4 - E_2)}{(E_3 - E_1)}, \tag{11}$$

thus providing a simple relation between the observed intensity ratio and the observed torsional splitting ratio.

III. RESULTS

The mm/submm techniques used for this experiment have been previously described (*14, 15*). Briefly, the output of a YIG oscillator is tripled and amplified by a traveling wave tube. Output from the TWT is matched onto a harmonic multiplier to generate multiples of the fundamental frequency. An InSb element cooled to liquid helium temperature is used to detect the microwaves. We have measured and assigned torsional splittings of 49 transitions in $2\nu_9$ and 95 transitions in ν_5. Assignments for the *R*-branch *b*-type and *Q*-branch *a*-type transitions are shown in Tables I and II for ν_5 and $2\nu_9$, respectively. We estimate the accuracy of these data to be 0.1 MHz or better.

TABLE I

Torsional Splittings of ν_5

J′	K'_-	K'_+	J″	K''_-	K''_+	ν(MHz)	J′	K'_-	K'_+	J″	K''_-	K''_+	ν(MHz)	Δ(MHz)
						R-Branch								
7	0	7	6	1	6	93 615.325	7	1	7	6	0	6	93 685.722	70.397
8	0	8	7	1	7	106 098.262	8	1	8	7	0	7	106 168.571	70.309
10	2	9	9	1	8	143 589.714	10	1	9	9	2	8	143 658.812	69.098
10	2	8	9	3	7	156 118.197	10	3	8	9	2	7	156 186.389	68.192
11	0	11	10	1	10	143 545.762	11	1	11	10	0	10	143 615.743	69.981
11	2	10	10	1	9	156 071.264	11	1	10	10	2	9	156 140.175	68.911
11	2	9	10	3	8	168 597.460	11	3	9	10	2	8	168 665.352	67.892
11	4	8	10	3	7	181 131.812	11	3	8	10	4	7	181 198.743	66.931
12	0	12	11	1	11	156 027.527	12	1	12	11	0	11	156 097.478	69.951
12	2	11	11	1	10	168 552.564								
12	2	10	11	3	9	181 077.020	12	3	10	11	2	9	181 144.539	67.519
13	0	13	12	1	12	168 508.928	13	1	13	12	0	12	168 578.738	69.810
13	2	12	12	1	11	181 033.505	13	1	12	12	2	11	181 102.000	68.495
14	0	14	13	1	13	180 989.851	14	1	14	13	0	13	181 059.564	69.713
						Q-Branch								
9	2	7	9	2	8	93 818.196	9	3	7	9	1	8	93 817.729	0.467
10	3	7	10	3	8	93 714.048	10	4	7	10	2	8	93 714.523	0.475
11	1	10	11	1	11	131 472.059	11	2	10	11	0	11	131 472.693	0.634
11	3	8	11	3	9	106 247.857	11	4	8	11	2	9	106 248.434	0.577
12	2	10	12	2	11	131 395.970	12	3	10	12	1	11	131 395.267	0.703
12	4	8	12	4	9	106 124.104	12	5	8	12	3	9	106 123.555	0.549
13	2	11	13	2	12	143 918.244	13	3	11	13	1	12	143 917.570	0.674
13	3	10	13	3	11	131 301.515	13	4	10	13	2	11	131 302.188	0.673
13	5	8	13	5	9	105 967.850	13	6	8	13	4	9	105 968.396	0.546
14	2	12	14	2	13	156 439.149	14	3	12	14	1	13	156 438.317	0.832
14	3	11	14	3	12	143 823.444	14	4	11	14	2	12	143 824.125	0.681
14	4	10	14	4	11	131 188.842	14	5	10	14	3	11	131 188.178	0.664
15	3	12	15	3	13	156 342.705	15	4	12	15	2	13	156 343.608	0.903
15	4	11	15	4	12	143 712.703	15	5	11	15	3	12	143 711.990	0.713
16	2	14	16	2	15	181 476.663	16	3	14	16	1	15	181 475.812	0.851
16	4	12	16	4	13	156 232.277	16	5	12	16	3	13	156 231.535	0.742
17	5	12	17	5	13	156 103.089	17	6	12	17	4	13	156 103.782	0.693
17	6	11	17	6	12	143 428.485	17	7	11	17	5	12	143 427.792	0.693
17	7	10	17	7	11	130 700.554	17	8	10	17	6	11	130 701.277	0.723
18	7	11	18	7	12	143 249.901	18	8	11	18	6	12	143 250.604	0.703
19	5	14	19	5	15	181 132.416	19	6	14	19	4	15	181 133.257	0.841
19	6	13	19	6	14	168 476.605	19	7	13	19	5	14	168 475.801	0.804
19	7	12	19	7	13	155 786.327	19	8	12	19	6	13	155 787.050	0.723
19	8	11	19	8	12	143 045.040	19	9	11	19	7	12	143 044.307	0.733
20	8	12	20	8	13	155 594.495	20	9	12	20	7	13	155 593.713	0.782
21	8	13	21	8	14	168 131.901	21	9	13	21	7	14	168 131.089	0.812
21	9	12	21	9	13	155 375.129	21	10	12	21	8	13	155 375.881	0.752
21	10	11	21	10	12	142 537.861	21	11	11	21	9	12	142 537.139	0.722
22	10	12	22	10	13	155 128.634	22	11	12	22	9	13	155 127.891	0.743
22	11	11	22	11	12	142 228.356	22	12	11	22	10	12	142 229.089	0.733
23	11	12	23	11	13	154 849.188	23	12	12	23	10	13	154 849.901	0.713
23	12	11	23	12	12	141 877.980	23	13	11	23	11	12	141 877.228	0.752
24	11	13	24	11	14	167 445.723	24	12	13	24	10	14	167 446.465	0.742
25	12	13	25	12	14	167 164.832	25	13	13	25	11	14	167 164.039	0.793

Splittings were initially observed on the Q-branch transitions for which the degeneracy of the a-type transitions was lifted resulting in two clearly resolvable spectral lines. For these transitions the selection rules are such that transitions are between either

TABLE II

Torsional Splittings of $2\nu_9$

J′	K'_-	K'_+	J″	K''_-	K''_+	ν(MHz)	J′	K'_-	K'_+	J″	K''_-	K''_+	ν(MHz)	Δ(MHz)
						R-Branch								
7	0	7	6	1	6	93 570.792	7	1	7	6	0	6	93 671.762	100.970
8	0	8	7	1	7	106 054.226	8	1	8	7	0	7	106 155.145	100.920
10	2	9	9	1	8	143 483.901	10	1	9	9	2	8	143 582.525	98.624
10	2	8	9	3	7	155 952.343	10	3	8	9	2	7	156 049.026	96.684
11	0	11	10	1	10	143 503.129	11	1	11	10	0	10	143 603.822	100.694
11	2	10	10	1	9	155 965.949	11	1	10	10	2	9	156 064.291	98.342
11	2	9	10	3	8	168 432.205	11	3	9	10	2	8	168 528.369	96.164
11	4	8	10	3	7	180 909.450	11	3	8	10	4	7	181 003.653	94.204
12	0	12	11	1	11	155 985.390	12	1	12	11	0	11	156 086.129	100.740
12	2	11	11	1	10	168 447.789								
12	2	10	11	3	9	180 912.444	12	3	10	11	2	9	181 008.119	95.676
13	0	13	12	1	12	168 467.569	13	1	13	12	0	12	168 568.189	100.620
13	2	12	12	1	11	180 929.356	13	1	12	12	2	11	181 027.111	97.756
14	0	14	13	1	13	180 949.297	14	1	14	13	0	13	181 049.871	100.574
						Q-Branch								
9	2	8	9	0	9	105 879.106	9	1	8	9	1	9	105 878.135	0.972
9	2	7	9	2	8	93 338.790	9	3	7	9	1	8	93 337.899	0.892
10	4	7	10	2	8	93 233.879	10	3	7	10	3	8	93 232.976	0.904
14	2	12	14	2	13	155 658.584	14	3	12	14	1	13	155 657.050	1.534
15	2	13	15	2	14	168 118.634	15	3	13	15	1	14	168 117.119	1.516
16	4	12	16	4	13	155 482.022	16	5	12	16	3	13	155 480.533	1.490
17	6	12	17	4	13	155 367.524	17	5	12	17	5	13	155 366.030	1.594
17	6	11	17	6	12	142 746.634	17	7	11	17	5	12	142 745.277	1.358
18	6	12	18	6	13	155 233.050	18	7	12	18	5	13	155 231.525	1.556
18	8	11	18	6	12	142 574.089	18	7	11	18	7	12	142 572.762	1.328
19	8	11	19	8	12	142 371.050	19	9	11	19	7	12	142 369.653	1.398

pairs of upper torsional states or lower torsional states. Thus, the observed splittings result from small changes of the torsional splitting with rotational state. Typical spectra for the $2\nu_9$ and ν_5 Q-branches are seen in Figs. 2 and 3, respectively. Additionally, it is clear from the Q-branch data in Tables I and II that the splitting itself has a functional dependence on K_+. This functional dependence is illustrated in Fig. 4, where the Q-branch splittings averaged over the individual K_+ branches are shown as a function of K_+, with the splittings varying from 0.97 to 1.55 MHz for $2\nu_9$ and from 0.47 to 0.90 MHz for ν_5.

Typical spectra for the R-branch transitions are shown in Figs. 5 and 6 for $2\nu_9$ and ν_5, respectively. The b-type transitions appear as a pair of smaller lines split symmetrically around the corresponding a-type transition seen in the center of each spectra. Here the a-type lines are between either pairs of upper or lower torsional states, but the selection rules are such that the changes between upper and lower state torsional splittings are too small to produce a splitting in the a-type transitions. However, the b-type spectra involve a torsional transition and represent a direct measure of the torsional splitting. These large splittings also show a functional dependence with quantum number. This dependence is shown in Figs. 7 and 8. A stronger dependence on

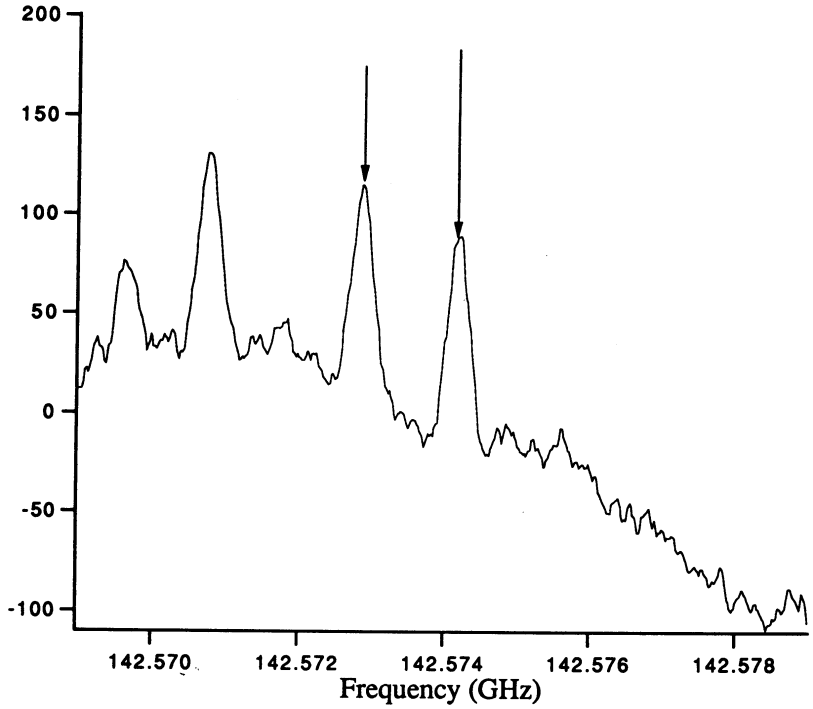

FIG. 2. Typical $2\nu_9$ Q-branch pair. Arrows indicate the torsionally split transitions.

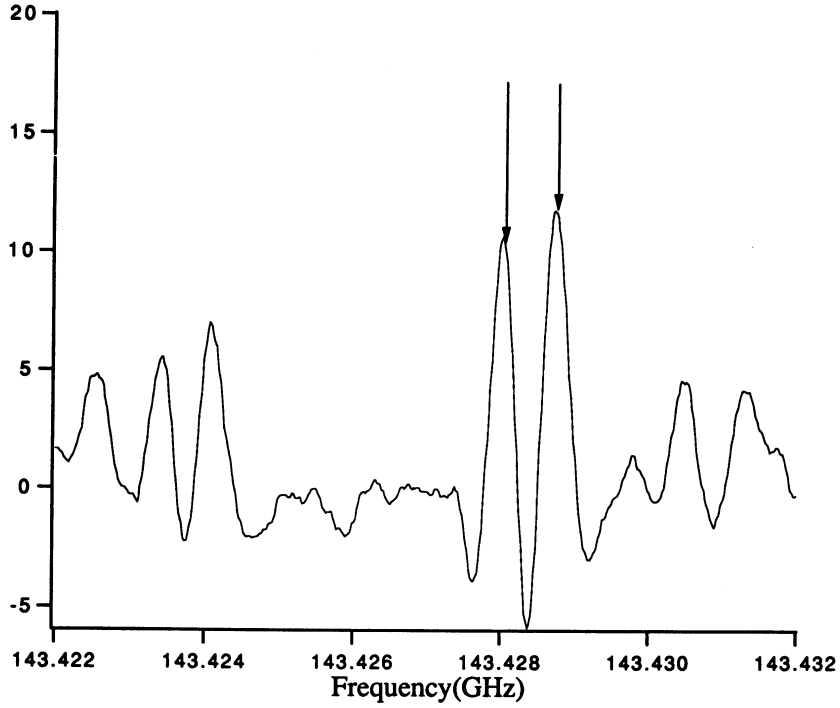

FIG. 3. Typical ν_5 Q-branch pair. Arrows indicate the torsionally split transitions.

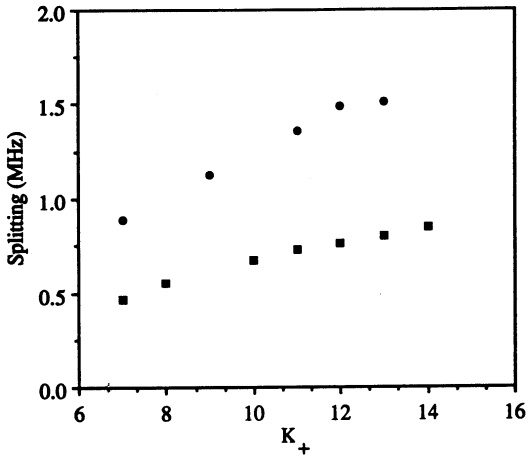

FIG. 4. Splitting between Q-branch transitions as a function of K_+ for $2\nu_9$ (circles) and ν_5 (squares).

K_- is seen with a weaker dependence on J, with the splitting between the b-type transitions varying from about 94 to 101 MHz for $2\nu_9$ and 67 to 70 MHz for ν_5. The splitting between the b-type lines represents twice the splitting of the energy levels in Fig. 1, since one transition is shifted up and one is shifted down by the same amount. It is interesting to note that the differences between the splittings from the different K levels is the same size as the Q-branch splittings. This result is expected since the Q-branchs are connected across levels of constant J, with K_+ differing by one.

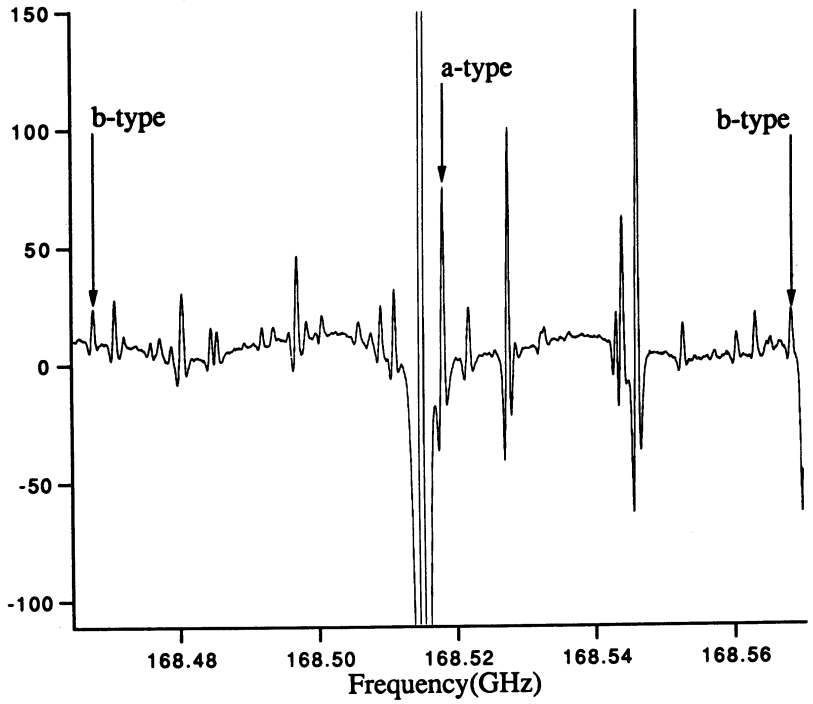

FIG. 5. Typical $2\nu_9$ R-branch spectra. The strong a-type and torsionally split b-type pair are indicated by arrows.

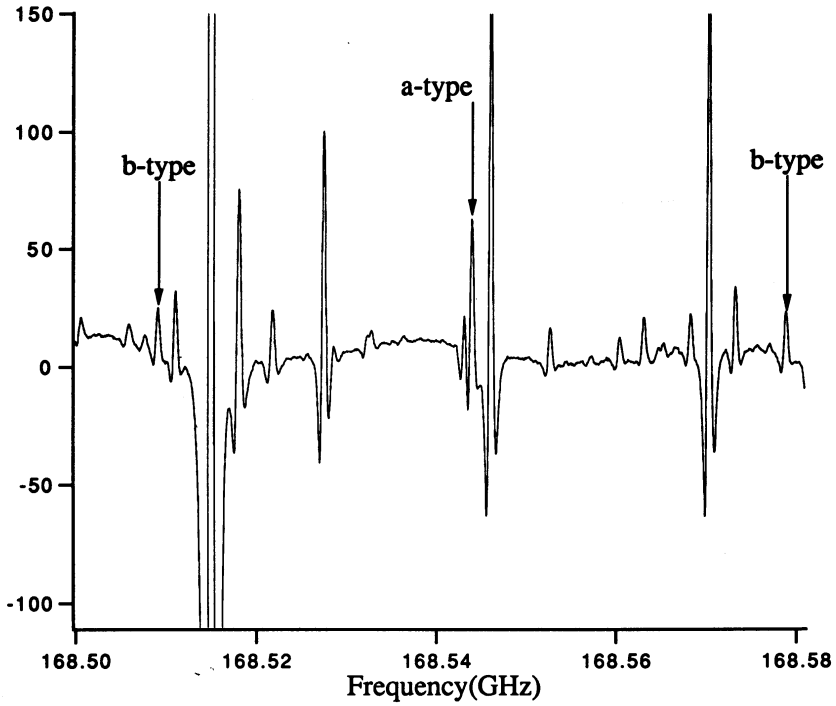

FIG. 6. Typical ν_5 R-branch spectra. The strong a-type and split b-type pair are indicated by arrows.

The data of Figs. 7 and 8 can be extrapolated to $J = 0$, yielding E_4–E_2 = 50.7 MHz and E_3–E_1 = 35.5 MHz, respectively. Substitution of these values into Eqs. (5) and using Eqs. (8)–(11) predicts the intensity ratio, rotation angle, Fermi interaction term and ΔE^0. We obtain the result that $\Gamma_{\nu_5}/\Gamma_{2\nu_9} = 1.43$, $\theta = 39.9°$, $W_{12} = 8.53\ \text{cm}^{-1}$, and $\Delta E^0 = 3.06\ \text{cm}^{-1}$. From the accuracy of our data we estimate these numbers to be good to 1%. Since $\Gamma_{\nu_5}/\Gamma_{2\nu_9}$ is in good agreement with the value of 1.4 reported in Ref.

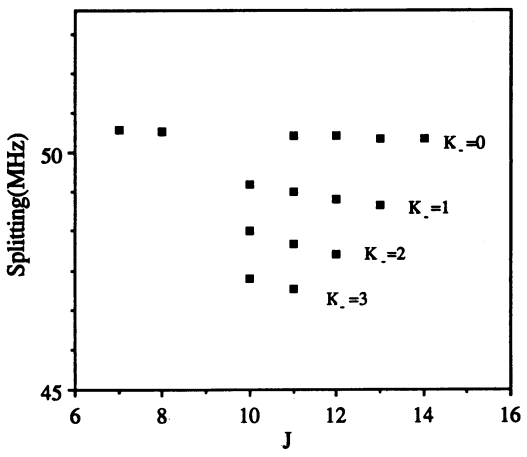

FIG. 7. Splitting of the $2\nu_9$ R-branch b-type transitions from the corresponding a-type transitions. Different K_- transitions are labeled.

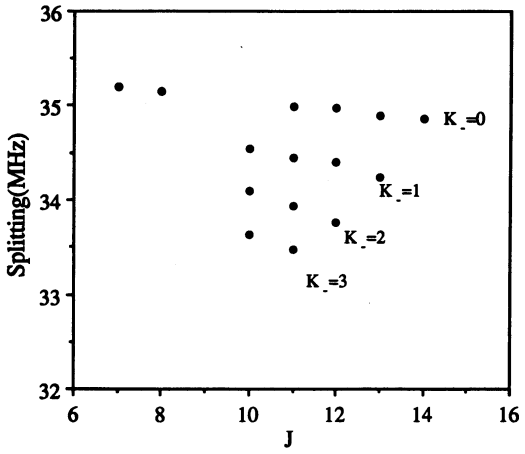

FIG. 8. Splitting of the ν_5 R-branch b-type transitions from the corresponding a-type transitions. Different K_- transitions are labeled.

(*1*), we conclude that to within experimental uncertainty in the infra-red intensity ratio, all of the $2\nu_9$ intensity in the infrared comes from mixing with ν_5, rather than from the intrinsic intensity of the $2\nu_9$ band.

IV. SUMMARY

Torsional splittings have been resolved and measured in both the ν_5 and $2\nu_9$ bands of HNO_3 by mm/submm spectroscopic techniques. The observed splitting of the ν_5 band results from a Fermi mixing of the two levels and can be used as a direct means of evaluating the mixing. From this analysis, it is possible to predict the observed intensity of the $2\nu_9$ band to within experimental uncertainty.

ACKNOWLEDGMENT

We would like to thank NASA for its support of this work.

RECEIVED: April 25, 1994

REFERENCES

1. A. PERRIN, V. JAOUEN, A. VALENTIN, J.-M. FLAUD, AND C. CAMY-PEYRET, *J. Mol. Spectrosc.* **157,** 112–121 (1993).
2. A. G. MAKI AND J. S. WELLS, *J. Mol. Spectrosc.* **152,** 69–79 (1992).
3. R. L. CROWNOVER, R. A. BOOKER, F. C. DE LUCIA, AND P. HELMINGER, *J. Quant. Spectrosc. Radiat. Transfer* **40,** 39–46 (1988).
4. D. G. MURCRAY, T. G. KYLE, F. H. MURCRAY, AND W. J. WILLIAMS, *J. Opt. Soc. Am.* **59,** 1131–1134 (1969).
5. P. E. RHINE, L. D. TUBBS, AND D. WILLIAMS, *Appl. Opt.* **8,** 1500–1501 (1969).
6. D. G. MURCRAY, D. B. BARKER, J. N. BROOKS, A. GOLDMAN, AND W. J. WILLIAMS, *Geophys. Res. Lett.* **2,** 223–225 (1975).
7. C. M. BRADFORD, F. H. MURCRAY, J. W. VAN ALLEN, J. N. BROOKS, D. G. MURCRAY, AND A. GOLDMAN, *Geophys. Res. Lett.* **3,** 387–390 (1976).
8. J. M. RUSSELL III, C. B. FARMER, C. P. RINSLAND, R. ZANDER, L. FROIDEVAUX, G. C. TOON, B. GAO, J. SHAW, AND M. GUNSON, *J. Geophys. Res. D* **93,** 1718–1736 (1988).
9. A. GOLDMAN, F. J. MURCRAY, R. D. BLATHERWICK, J. J. KOSTERS, F. H. MURCRAY, D. G. MURCRAY, AND C. P. RINSLAND, *J. Geophys. Res. D* **94,** 14945–14955 (1989).

10. C. P. RINSLAND, R. ZANDER, AND P. DEMOULIN, *J. Geophys. Res. D* **96,** 9379–9389 (1991).
11. T. GIESEN, M. HARTER, R. SCHIEDER, G. WINNEWISSER, AND K. M. T. YAMADA, *Z. Naturforsch. A* **43,** 402–406 (1988).
12. C. H. TOWNES AND A. L. SCHAWLOW, "Microwave Spectroscopy," pp. 35–40, McGraw–Hill, New York, 1975.
13. J. OVEREND, *in* "Infrared Spectroscopy and Molecular Structure" (M. Davies, Ed.), pp. 345–353, Elsevier, New York, 1963.
14. P. HELMINGER, J. K. MESSER, AND F. C. DE LUCIA, *Appl. Phys. Lett.* **42,** 309–310 (1983).
15. R. A. BOOKER, R. L. CROWNOVER, F. C. DE LUCIA, AND P. HELMINGER, *J. Mol. Spectrosc.* **128,** 62–67 (1988).